Published in final edited form as:
Exp Eye Res. 2008 February ; 86(2): 434–444.

Analysis of nuclear fiber cell cytoplasmic texture in advanced cataractous lenses from Indian subjects using Debye-Bueche theory

S. Metlapally[a], **M. J. Costello**[a], **K. O. Gilliland**[a], **B. Ramamurthy**[b], **P. V. Krishna**[b], **D. Balasubramanian**[b], and **S. Johnsen**[c]

a*Department of Cell and Developmental Biology, University of North Carolina, Chapel Hill, NC*

b*L. V. Prasad Eye Institute, Hyderabad, India*

c*Department of Biology, Duke University, Durham, NC.*

Abstract

Alterations in ultrastructural features of the lens fiber cells lead to scattering and opacity typical of cataracts. The organelle-free cytoplasm of the lens nuclear fiber cell is one such component that contains vital information about the packing and organization of crystallins critical to lens transparency. The current work has extended analysis of the cytoplasmic texture to transparent and advanced cataractous lenses from India and related the extent of texturing to the nuclear scattering observed using the Debye-Bueche theory for inhomogeneous materials. Advanced age-related nuclear cataracts (age-range 38–75 years) and transparent lenses (age-range 48–78 years) were obtained following extracapsular cataract removal or from the eye bank, at the L. V. Prasad Eye Institute. Lens nuclei were Vibratome-sectioned, fixed and prepared for transmission electron microscopy using established techniques. Electron micrographs of the unstained thin sections of the cytoplasm were acquired at 6500X and percent scattering for wavelengths 400–700 nm was calculated using the Debye-Bueche theory. Electron micrographs from comparable areas in an oxidative-damage sensitive (OXYS) rat model and normal rat lenses preserved from an earlier study were used, as they have extremely textured and smooth cytoplasms, respectively. The Debye-Bueche theoretical approach produces plots that vary smoothly with wavelength and are sensitive to spatial fluctuations in density. The central lens fiber cells from advanced cataractous lenses from India and the OXYS rat, representing opaque lens nuclei, produced the greatest texture and scattering. The transparent human lenses from India had a smoother texture and less predicted scattering, similar to early cataracts from previous studies. The normal rat lens had a homogeneous cytoplasm and little scattering. The data indicate that this method allowed easy comparison of small variations in cytoplasmic texture and robustly detected differences between transparent and advanced cataractous human lenses. This may relate directly to the proportion of opacification contributed by the packing of crystallins. The percent scattering calculated using this method may thus be used to generate a range of curves with which to compare and quantify the relative contribution of the packing of crystallins to the loss of transparency and scattering observed.

Corresponding author: M. J. Costello, PhD, Department of Cell and Developmental Biology, University of North Carolina at Chapel Hill, Chapel Hill, North Carolina 27599-7090., (ph): +1-919-966-6981 (fax): +1-919-966-1856, (email):mjc@med.unc.edu.

Keywords

aged; lens nucleus; cataract; cytoplasm; humans; scattering; electron microscopy; Fourier analysis

1. Introduction

The ocular lens is designed to be transparent and transmits visible light to the retina with negligible absorption and scattering. Transparency of the ocular lens depends primarily on its ultrastructure. The lack of cellular organelles along the light path (Bassnett, 2002), close packing of fiber cells to minimize extracellular space (Taylor et al., 1996), organization of its predominant component proteins (crystallins) (Bettelheim and Siew, 1983; Delaye and Tardieu, 1983) and the conspicuous absence of large fluctuations in refractive index contribute to this crucial feature of the lens (Benedek, 1971; Bettelheim, 1985; Zigler, 1994; Kuszak and Costello, 2004). Cataract, defined as any opacity of the lens, is characterized by overall diminished contrast at the retina due to both absorption and increased scattering of incident light leading to visual deficit (Duncan, 1981; Brown and Bron, 1996; Datiles and Magno, 2004; Costello and Kuszak, 2007). Age-related nuclear cataracts, the most common form of human cataracts (Murthy et al., 2007), begin as white hazy scattering in the nuclear core and progressively involve more of the nucleus as the cataract matures. Ultrastructural features that have been reported from our laboratory to be contributory to the scattering and opacity of human lens nuclei include enlarged extracellular spaces, extracellular space deposits (Costello et al., 1992; Al-Ghoul et al., 1996), distinct 1–4 μm globular particles called multilamellar bodies (Gilliland et al., 2001; Gilliland et al., 2004) and texturing of fiber cell cytoplasm seen in thin sections (Al-Ghoul and Costello, 1996; Taylor and Costello, 1999; Freel et al., 2002).

An important observation from these ultrastructural studies was that early or immature age-related nuclear cataracts were similar in morphology to transparent non-cataractous lenses (Al-Ghoul and Costello, 1996; Al-Ghoul et al., 1996; Kuszak et al., 1998; Freel et al., 2002), except for a greater number of large scattering particles, the multilamellar bodies (Gilliland et al., 2001; Gilliland et al., 2004). However, few such detailed comparisons have been possible with advanced cataracts due to methodological reasons, especially problems of availability and adequate fixation of the interior of the dense ocular lens. The study of advanced age-related nuclear cataracts may provide valuable data regarding the physical basis of transparency and the mechanisms of cataract formation, and may corroborate or invalidate widely held theories about these aspects of lens research. Moreover, this may also provide us with clues for delaying the onset of cataract or addressing the critical need to devise preventative strategies for cataract, which is the leading cause of blindness in the world, particularly in developing countries (Thylefors et al., 1995; Dandona et al., 2001; Foster, 2001; Nirmalan et al., 2003).

The current study has concentrated specifically on the ultrastructure of cytoplasmic texturing seen in dehydrated and embedded thin-section micrographs of nuclear tissue from advanced age-related cataracts. This feature is directly related to the packing, density and organization of crystallins within lens fiber cells. Biochemical studies have reported that crystallins aggregate into high-molecular-weight particles (Jedziniak et al., 1973; Spector and Roy, 1978; Zigler, 1994; Benedek, 1997) and this is generally accepted to be the underlying cause of scattering seen in nuclear cataracts. The size of these presumably distinct particles, in theory, should be in the range 20–200 nm to produce significant scattering (Benedek, 1971; Bettelheim, 1985; Clark, 1994), a size range that can be visualized easily in thin-section electron micrographs. Yet, high-molecular-weight aggregate particles have not been observed within the cytoplasm of well-preserved human nuclear fiber cells (Costello et al., 1992; Al-Ghoul and Costello, 1996; Al-Ghoul et al., 1996; Taylor and Costello, 1999; Freel et al., 2002). Fourier analysis has been used to quantify cytoplasmic texturing in age-related nuclear cataracts

(possibly from protein modification or redistribution) and to relate it to the scattering (Taylor et al., 1997; Taylor and Costello, 1999; Freel et al., 2002; Costello and Johnsen, 2004), as the technique is sensitive to small variations not perceived by eye. Results from these studies show that the cytoplasm in mild age-related cataracts is similar to age-matched transparent lenses and in these instances cytoplasmic variations do not account entirely for the observed scattering.

An extension of detailed ultrastructural analyses to more advanced age-related nuclear cataracts extracted during surgery from blind subjects in India has offered preliminary information regarding the innermost fiber cells (Costello et al., 2006). In the current study, we have estimated the contribution of the packing and organization of the fiber cell cytoplasm to light scattering from the in vivo lens nucleus in transparent lenses to lenses with a range of opacities. The well-established Debye-Bueche theory for inhomogeneous materials (Debye and Bueche, 1949) has been used in this analysis, as has been used in the past for characterizing scattering from the lens (Bettelheim and Paunovic, 1979; Bettelheim et al., 1981; Bettelheim and Siew, 1983), because this theory is robust and directly applicable to thin sections of densely packed amorphous proteins. The analysis indicates that the organization of the cytoplasm is altered markedly in advanced age-related nuclear cataracts and is a major contributor to the total light scattering by cataractous nuclei.

2. Materials and Methods

2.1. Lens material

Lens nuclei from advanced age-related nuclear cataracts (graded 3–4 on a 0–4 scale by clinicians; n=10) were obtained from subjects in the age range 38 to 75 years, who underwent extracapsular cataract extractions at L. V. Prasad Eye Institute, Hyderabad, India. The nuclei were brought from the operating room to a laboratory in the facility in a vial containing gauze moistened with saline at room temperature immediately following extraction. Patient information obtained was limited to the age, gender, diabetes mellitus status and the nuclear cataract grading by the surgeon, following guidelines of the Institutional Review Board for protection of human subjects. Transparent whole donor lenses (n=4; age-range 48–78) obtained from the Ramayamma International Eye Bank located within the Institute had limited information available, usually only the age and gender. All lenses were obtained according to the tenets of the Declaration of Helsinki. Oxidation sensitive (OXYS) (n=1) and normal rat (n=1) lenses preserved from earlier studies (Marsili et al., 2004) were used for comparison.

2.2. Fixation and sectioning

Lenses obtained were examined using a hand-held slit lamp (model 510, Eidolon Corporation, MA, USA) and had their equatorial diameters and thicknesses measured using calipers. They were sectioned into 200 μm thick slices using a Vibratome (series 1000, St.Louis, MO, USA). The freshly cut slices were then prepared as described in earlier studies (Freel et al., 2002). In brief, they were immersed in modified Karnovsky's fixative (2.5% gluteraldehyde, 2% paraformaldehyde and 1% tannic acid in 0.1 M sodium cacodylate buffer, pH 7.2) for 12–18 hours, washed in 0.1 M cacodylate buffer three times, treated with 0.5% osmium tetroxide for one hour at 4° C, washed with deionized distilled water, washed in 50% ethanol, and *en bloc* stained in the dark with 2% uranyl acetate dissolved in 50% ethanol, followed by dehydration in a graded ethanol series. The sections were then infiltrated and embedded in epoxy resin. Thin-section mesas were raised along the optic axis to include the embryonic and inner fetal nuclear fiber cells and sections with thickness ranging from 50–70 μm were cut using a diamond knife (Diatome US, Fort Washington, PA, USA). The sections thus collected on copper grids were not grid-stained with uranyl acetate or lead citrate by design. They were

visualized at 80 kV using an FEI-Philips Tecnai 12 (FEI Company, Hillsboro, OR, USA) transmission electron microscope (TEM).

2.3. Cytoplasm Image collection

Representative images for all the lenses (1024×1024 pixels, equating to approximately 2.6 μm^2 area) of the cytoplasm within different embryonic or inner fetal lens nuclear fiber cells were collected at a magnification of 6500X using a Gatan digital camera (Gatan Inc., Pleasanton, CA, USA; model 794, 1024×1024 pixel CCD located below the image plane) and Digital Micrograph software (v. 3.9.3, Gatan Inc.). These images were collected with care, avoiding features that could confound calculations like membranes, compression bands, knife marks and other known variations due to sample preparation. Fourier analysis was carried out on each of these images using the fast Fourier transform algorithm of Digital Micrograph software, the basis and theory of which have been discussed in earlier publications (Taylor and Costello, 1999; Freel et al., 2002). Fourier analysis also helped detect obvious defocus or imperfections undetectable by the naked eye in these relatively low-contrast images during their collection and such images were not used in the analyses.

2.4 Theoretical treatment

From Debye and Bueche (1949), the intensity of light scattered from a tissue at an angle θ is given by

$$i(\theta) = \frac{I}{r^2}\frac{\pi^2}{\varepsilon^2\lambda^4}\frac{1+\cos^2\theta}{2}V\bar{\eta}^2\omega(\theta), \tag{1}$$

where I is the intensity of the incident light, r is the distance from the tissue that the scattered light is measured, and λ is the wavelength of the incident light in the tissue. V is the volume of the tissue and $\bar{\eta}^2$ is the average squared fluctuation from its average dielectric constant ε (equal to square of the average refractive index). The correlation volume ω(θ) is given by

$$\omega(\theta) = 4\pi\int_0^\infty s^2\gamma(s)\frac{\sin(\mathrm{hs})}{\mathrm{hs}}\mathrm{ds}, \text{ where } h = \frac{4\pi}{\lambda}\sin\left(\frac{\theta}{2}\right). \tag{2}$$

The function γ(*s*) is the radial autocorrelation function of the fluctuations of the dielectric constant and is given by

$$\gamma(s) = \frac{1}{\bar{\eta}^2 N_s}\sum_{\sqrt{x^2+y^2}=s} A(x,\ y), \tag{3}$$

where N_s is the number of points with coordinates *(x,y)* that are a distance *s* from the origin of the autocorrelation image *A*. *A* is equal to the modulus of the Fourier transform of the modulus of the Fourier transform of the fluctuations of the dielectric constant of the tissue, or

$$A(x,\ y) = \left|\Im\left\{\left|\Im\{\eta(x,\ y)\}\right|\right\}\right|. \tag{4}$$

The average squared fluctuation of dielectric constant $\bar{\eta}^2$ (which also equals *A(0,0)*) is in the denominator of (3) so that γ(0) = 1.

The total scattered light over all angles is equal to

$$S_{\text{total}} = 2\pi\int_0^\pi i(\theta)r^2\sin\theta d\theta. \tag{5}$$

If one assumes that the illuminated tissue is spherical with a radius *R*, the total incident light flux equals the incident intensity times the cross-sectional area of the tissue, or

$$I_{\text{total}} = I\pi R^2, \tag{6}$$

so, the fraction of light scattered equals

$$\frac{S_{\text{total}}}{I_{\text{total}}} = \frac{2\pi\int_0^{\pi} i(\theta) r^2 \sin\theta d\theta}{I\pi R^2} = \frac{4\pi^3 \bar{\eta}^2 R}{3\varepsilon^2 \lambda^4} \int_0^{\pi} (1 + \cos^2\theta)\omega(\theta)\sin\theta d\theta. \quad (7)$$

2.5 Image processing

TEM staining intensity has been used as an indicator of protein density and refractive index by many researchers (Gisselberg et al., 1991; Vaezy and Clark, 1994; 1995; Vaezy et al., 1995; Taylor et al., 1997; Taylor and Costello, 1999; Clark, 2001). This is because heavy metal stains used in electron microscopy are generally non-specific (Glauert, 1965; Hayat, 1971) and refractive index is linearly proportional to density and relatively independent of the actual molecule (Michielsen, 1999). We have employed the stain density-refractive index relationship because it is the only available method of estimating refractive index at optical wavelengths using non-optical techniques at electron microscopy resolution (Marsili et al., 2004).

In the current study, representative electron micrographs from all lenses used had a 1024 × 1024 region of interest (ROI) selected. The refractive index of white pixels was set equal to that of cytoplasm, 1.35 (Charney and Brackett, 1961), and the refractive index of black areas was set to be that of dense protein, 1.51 (Philipson, 1973; Freegard, 1997), as described previously by Marsili et al. (2004). These values were then squared to create an image of the distribution of the dielectric constant ε. The average dielectric constant of the image was then subtracted from it, to create an image of the fluctuations of ε. The average squared fluctuation of the dielectric constant $\bar{\eta}^2$ was calculated by averaging the squares of all the values in the fluctuation image. The fluctuation image was then multiplied by a Hanning window function (Diniz et al., 2002). This function reduces the amplitude of the spatial variation of the fluctuations as they approach the edge of the ROI. It is done because the Fourier transform used in this analysis assumes that the ROI wraps around at all edges (i.e., is a torus) and thus gives spurious frequencies due to the sharp discontinuities at the edges. The windowed image was then converted to an auto-correlation image $A(x,y)$ by taking the modulus of the transform of the modulus of the transform, using the Fast Fourier Transform (FFT) algorithm. The auto-correlation image was then converted to the linear function $\gamma(s)$ by averaging all the values at given distances from the center of the image and then dividing by $\bar{\eta}^2$ (so that $\gamma(0) = 1$). Values of the normalized function $\gamma(s)$ that were less than 0.005 were set to zero. This value was chosen because it approximated the noise floor of the Fourier transforms. Finally, values of $\gamma(s)$ for s>200 nm were set to zero. The assumption behind this was that any fluctuations greater than 200 nm in extent were artifactual (due to staining variation, etc.) and not related to cytoplasmic protein packing. This modified $\gamma(s)$ and the constants ε and $\bar{\eta}^2$ were then inserted into equation (7) to solve for percent scattered light as a function of wavelength (from 400 to 700 nm). The Debye-Bueche theory assumes spherical symmetry, and therefore percent scattering was determined for a spherical nuclear cataract. The volume of the human embryonic and fetal lens nuclear regions examined was considered to be 24 mm^3 for this calculation (Gilliland et al., 2001). The radius of the sphere and therefore the cross-sectional area were calculated from this known volume, followed by the scattered intensity at all angles. The photons scattered at all angles were obtained by integrating these scattered intensities and this was divided by the product of the incident intensity and the cross-sectional area to obtain percent scattering. Percent scattering from cytoplasmic images of cataracts were averaged to make statistical comparisons with results obtained from transparent human lenses.

2.6 Statistics

Representative images from ten advanced cataractous lenses and four transparent donor lenses from India were used to calculate percent scattering as described above. The area under each curve was obtained by numerical integration over 400–700 nm using the trapezoidal rule for

numerical integration. The results were then compared between cataractous and transparent Indian lenses using unpaired student t-test.

3. Results

3.1. Structure of lens nuclear fiber cells in advanced age-related cataracts from India

The lens nuclei from advanced age-related nuclear cataracts were studied using various techniques. The average equatorial diameter of nuclei used in this study was 7.9 mm, indicating that most of the entire adult nucleus was available. Gross morphological appearance revealed that most of these nuclei were fully opaque when examined with a hand-held slit lamp. Low magnification views of cellular morphology and cytoplasmic texture visible in thin-section micrographs from Indian cataractous lens nuclear fiber cells (figure 1A) were essentially identical to transparent Indian lens nuclear fiber cells (figure 1B) and nuclear cataracts from the United States (Costello et al., 1992; Al-Ghoul et al., 1996), showing uniform staining of the cytoplasm and cell interfaces, seen in these figures as white lines with various simple and complex cellular profiles.

3.2. Nuclear fiber cell cytoplasmic texture

Images of the cytoplasm within nuclear fiber cells at 6500X magnification revealed visible differences in the cytoplasmic texture between the cataractous and transparent lenses in micrographs collected from these lenses. The cataracts showed considerable texturing of the cytoplasm as seen in representative images; however, the supposed high-molecular-weight aggregates were not visualized as distinct particles (figures 2A, 2B, 2C). In comparison transparent Indian donor lenses showed minor texturing and essentially appeared smooth (figure 2D). The cytoplasm within OXYS rat lens fiber cells appeared much more textured at this magnification (figure 2E) and concurred with similar findings reported in previous studies (Freel et al., 2002; Marsili et al., 2004). The normal rat lens cytoplasm had the smoothest appearance (figure 2F), also in agreement with earlier observations (Freel et al., 2002; Marsili et al., 2004).

Percent scattering is plotted as a function of wavelength (figure 3). Each curve showed a decrease in percent scattering with increasing wavelength as described before for the lens (van den Berg, 1997). Consequently, plots show a greater spread in the blue end of the spectrum (shorter wavelengths) compared to the red end, although the ratios are probably nearly constant. Also, an important advance from previous studies by Marsili et al. (2004) and Costello and Johnsen (2004) was that there were no rapid fluctuations in the calculations due to use of the Hanning function and the removal of artifactual fluctuations greater than 200 nm in size using filters.

In general, advanced human cataracts showed significantly higher predicted scattering than transparent human lenses ($p<0.01$, unpaired t-test, figure 3), implying significant opacification. This was compatible with the crude observations of higher texturing seen in micrographs of cataracts compared to transparent lenses from India (figures 2A, 2B, 2C vs. 2D). In addition, the OXYS rat model showed the greatest percent scattering, also representing an opaque lens. The data from the OXYS rat were in agreement with observations from micrographs and from previous studies as well (Freel et al., 2002). Normal rat lenses which were observed to have the smoothest cytoplasm by eye demonstrated the least predicted scattering as before (Freel et al., 2002;Marsili et al., 2004). These calculations were made for the contribution of the scattering seen from the cells in the innermost developmental regions of the human lens and generalized to the scattering from the entire volume of these regions (calculated to be 24 mm^3).

The data for the Indian cataracts have been averaged (figure 4) and reveal the same general trends, with the cataractous tissue scattering more than the transparent human lens tissue. The average Indian cataract from this study shows approximately 8 times more scattering than the Indian transparent lens. These values for percent scattering from the embryonic and fetal nuclear regions of the lens are intended to be compared on a relative scale and are not absolute values for in vivo lens tissue.

The cytoplasm from the fiber cells within cataracts and the transparent lens (figures 2A, 2C and 2D, respectively) were analyzed and plotted as three dimensional graphs in figures 5A, 5B and 5C to better understand the scattering in relation to the scattering angles. The scattering, represented here as Rayleigh ratios, has been plotted against the scattering angle and the wavelength of incident light in the visible region (400–700 nm). The cataract represented in figure 2A demonstrated high percent scattering (figure 3-yellow line) and showed large-scale fluctuations that resembled fluctuations caused by disturbances approaching 200 nm in size, based on the large amount of light scattered at low angles (figure 5A). This implies a considerable opacification due to the textural disturbances in the cytoplasm alone. In comparison, the cataract represented in figure 2C demonstrated intermediate percent scattering (figure 3-green line) and demonstrated moderate fluctuations of the cytoplasm that showed no tendency for scattering at low or high angles (figure 5B). In this case, it is possible that opacification is either modest or has contributions from other components of the lens (e.g., membranes and multilamellar bodies). The plot from a representative transparent donor lens (figure 2D, figure 3-black line) was essentially even and horizontal (figure 5C), implying negligible scattering due to fluctuations in the cytoplasm.

4. Discussion

The current study preserved the oldest fiber cells (embryonic and fetal nuclei) in advanced nuclear cataracts from India to study the texture of the fiber cell cytoplasm in electron micrographs using the Debye-Bueche theory. The results indicate that the methods were successful in relating the cytoplasmic texture to the predicted scattering, also a measure of opacity. The results also suggest that the predicted scattering based on cytoplasmic texture is directly related to the extent of cataract formation, as advanced cataracts evaluated in this study (higher nuclear cataract grades) were found to have predicted scattering values considerably different from transparent donor lenses.

Advanced age-related nuclear cataracts, in this instance from blind subjects in India, have been evaluated for the first time using previously established methods for preserving the interiors of the dense, impermeable ocular lens (Costello et al., 1992; Al-Ghoul and Costello, 1996; Freel et al., 2002). Preliminary information obtained reveals that these advanced Indian cataracts are similar in their overall cell structure to less advanced cataracts obtained from the United States and examined in earlier studies (Costello et al., 2006). The differences appear to lie mainly in the extent of cataract maturity and not in any feature unique to lenses from India. This implies that lenses respond similarly to stress in both populations, although perhaps the extent of damage is greater over a shorter duration of time because of either greater intrinsic susceptibility of the Indian population to known stresses or the potency of environmental cataractogenic factors in India and their interactions with this susceptibility.

While the exact nature of the stresses encountered by each lens examined is difficult to determine, multiple factors are likely to be involved, resulting, among other outcomes, in increased cytoplasmic texture in mature cataracts. Biochemical evidence indicates that high-molecular-weight aggregates exist (Jedziniak et al., 1973; Jedziniak et al., 1975; Spector and Roy, 1978; Zigler, 1994) and that they are potential sources of scattering in the cytoplasm. However, as noted above, they were not found as distinct particles in the current or previous

ultrastructural studies (Costello et al., 1992; Freel et al., 2002; Freel et al., 2003; Costello and Johnsen, 2004). The filters used in the calculations ensured that aggregates in the size range most likely encountered in the cytoplasm (20–200 nm) were analyzed. The use of filters was reasonable in view of the fact that scattering curves obtained were smooth, providing consistent and meaningful results for the visible wavelengths of light. Comparison with the transparent human lenses from India for these calculations further emphasized the contributions of cytoplasmic complexity towards predicted scattering, revealing differences on a relative scale. The images used in these calculations were chosen from well-preserved regions of the inner fetal and embryonic nucleus. It is possible that the texture varied for different cells within each nucleus, if, for instance, older cells in the embryonic nucleus were more damaged than those in the fetal nucleus. This feature has not been explored systematically in the current study, although it may explain some of the variability in the predicted scattering based on cytoplasmic textural variations.

Fourier analysis provides us with a powerful tool to analyze variations not readily visualized by eye and has been used successfully in earlier studies to characterize the fluctuations seen in the fiber cell cytoplasm (Freel et al., 2002; Freel et al., 2003; Costello and Johnsen, 2004; Marsili et al., 2004). The preservation of a variety of textures from human and animal lenses suggests that the chemical fixation procedures have stabilized the native protein distributions. This conclusion is supported by using high-pressure freezing as the initial fixation step, followed by freeze-substitution, which produces similar patterns of protein distribution to conventional chemical fixation (Costello, 2006). The important difference in the current study is that the Fourier transforms of images are used as inputs into the Debye-Bueche equation to predict scattering in advanced age-related cataracts that have not been studied previously.

Previously, Debye-Bueche analysis, referred to as the ‘random fluctuation theory,’ was performed on the scattering from transparent human lenses (Bettelheim and Paunovic, 1979). They included an extension of the theory for the evaluation of orientation fluctuations that might detect anisotropic structures, such as bundles of cytoskeletal elements (Bettelheim and Paunovic, 1979). The calculated correlation functions were determined from scattering curves of frozen-thawed sections of lenses cut at different depths perpendicular to the optic axis. The correlation functions were interpreted in terms of high-molecular-weight protein aggregates dispersed in a medium of lower average refractive index. The most important findings were that the density fluctuations predominated (much larger than orientation fluctuations) and that the average size of the aggregates for aged lenses was about 300–450 nm with an average separation of about 400 to 1200 nm (Bettelheim and Paunovic, 1979). This approach was also applied to human cataractous lenses (Bettelheim et al., 1981; Siew et al., 1981). All lenses showed increased scattering in the nucleus and were considered to be nuclear cataracts based on the photographic evaluation (Chylack et al., 1981; Siew et al., 1981). There was reasonably good correlation of the regions of opacity in the intact cataracts with the regions of greatest density fluctuations. The average aggregate protein size was predicted to be about 250–500 nm with separations from 400 to 1800 nm. The most consistent finding was that the density fluctuations were more prominent than orientation fluctuations and that considerable variability among cataracts suggested that each cataract had distinguishing characteristics. It is worth noting that the orientation fluctuations showed rapid changes at the cortex/nucleus interface, where cell compaction is evident, and in the central nucleus where the anisotropy probably involves the membranes, because no cytoskeletal elements are present (Bettelheim and Paunovic, 1979; Bettelheim et al., 1981). In the current study we have emphasized only the density fluctuations and have imaged cytoplasm only in regions without membranes, thus avoiding anisotropic features that could contribute to the orientation fluctuations. Furthermore, the calculation of predicted scattering does not depend on a molecular interpretation of the scattering patterns. Even in the absence of high-molecular-weight aggregates as distinct

particles, differences in density fluctuations appear to be sufficient to distinguish the cataracts and produce a wide range of calculated scattering intensities.

The Debye-Bueche analysis was also employed to examine the influence of concentration on scattering in model systems of condensed protein solutions (Bettelheim and Siew, 1983). It was shown that as the concentration increased beyond a certain threshold, the calculated scattering began to decrease. This concentration effect was clearly demonstrated for isolated bovine cytoplasm by Delaye and Tardieu (1983). These two papers support the idea that destructive interference of scattered light rays increases as the scattering units become closely packed with only short-range order and this pattern is the basis for the transparency of fiber cell cytoplasm. Conversely, it is implied that dilution of the crystallins will increase scattering; however, dilution would not normally be possible within the human lens nucleus where dehydration is maintained during aging and cataract formation. It has been suggested that the driving force behind the dehydration of the nuclear cytoplasm is the self-association and aggregation of crystallins leading to fewer mobile components and to a greatly reduced osmotic stress (Tardieu et al., 1992; Kenworthy et al., 1994). This close association and aggregation of crystallins occurs normally and accounts for the hardening of the nucleus in most non-primate animal models that do not rely on accommodation. In humans the hardening of the nucleus is delayed for about four decades, but it should be emphasized that nuclear hardening during the onset of presbyopia usually precedes the formation of age-related nuclear cataracts (McGinty and Truscott, 2006).

This raises the question of how a densely packed and dehydrated nuclear cytoplasm can produce excess light scattering. The commonly held view is that the extensive post-translational modification of crystallins produces high-molecular-weight aggregates that have a higher refractive index and scatter light (Benedek, 1997). The evidence for the existence of the high-molecular-weight aggregates is compelling (Jedziniak et al., 1973; Jedziniak et al., 1975; Spector and Roy, 1978) and their role in normal lens aging and cataract formation is critical. Limited morphological evidence indicates that individual aggregates are irregular assemblies of smaller subunits in isolated nuclear cytoplasm from bovine (Kramps et al., 1975; Siezen et al., 1979), rabbit (Liem-The et al., 1975) and human (Costello and Kuszak, 2007) lenses. However, the morphology of the intact cytoplasm suggests that the aggregates assemble into a complex three-dimensional network of closely packed protein with smaller more mobile crystallins filling in spaces to create a homogeneous cytoplasm. This current study of advanced cataracts from India suggests an alternative explanation of cataract formation. Because the low magnification views of nuclear fiber cell cytoplasm appear smooth and high magnification views do not reveal high-molecular-weight particles, the modifications of crystallins (Lampi et al., 1998; Hanson et al., 2000; Truscott, 2005) may release cytoplasmic components from the dense network. The loss of material at local sites would produce low-density regions (holes or voids) that are not filled in with other proteins because the components of the network in aged lenses are relatively immobile. The result would be fluctuations in density and in refractive index that could account for the increased scattering demonstrated here using the Debye-Bueche analysis.

For this study, a change in the data collection procedure has given a better overview of cytoplasmic texture. Earlier studies from our laboratory sampled a smaller area while collecting micrographs for such analysis (using a higher magnification of 21000X), unlike the larger area sampled in the current study (magnification 6500X). We considered the chosen magnification sufficient to collect images of the cytoplasm from the relatively large cells in the embryonic and fetal nucleus without interference from membranes or areas containing other procedurally induced imperfections, allowing us to examine data from larger contiguous regions. Also, a key assumption of the Debye-Bueche theory is that the scattering predicted from cells in the inner core of the lens nucleus, when applied to the nuclear volume representative of these cells

as done in the current study, gives us a measure of opacity. The predicted scattering in the current study has been calculated for a spherical volume as an approximation to the actual ellipsoid shape and is used for comparisons on a relative scale. In addition, it should be noted that the contributions of lens fiber cell membranes and multilamellar bodies are not accounted for in these calculations. This is beneficial in the study of scattering and opacity of the lens, because it allows separation of the contributions of each of these components to scattering using different theories that account for their unique properties.

The results indicate that advanced cataracts show a greater texture and are estimated to scatter a larger proportion of the incident light than immature cataracts and transparent lenses. As mentioned before, this relates directly to the packing, density and organization of the crystallins. An increased texturing may therefore signify modifications of the crystallins due to aging changes, leading to the loss and/or redistribution of the cytoplasmic components, causing refractive index fluctuations and scattering (Al-Ghoul and Costello, 1996; Taylor and Costello, 1999). The fundamental goal then is to demonstrate that all advanced cataracts of the common type, i.e., age-related nuclear, have similar features and accumulate evidence for the hypothesis regarding the loss and/or redistribution of cytoplasmic protein. A large body of biochemical evidence points to modifications of the crystallins (Zigler, 1994; Lampi et al., 1998; Ma et al., 1998; Hanson et al., 2000; Truscott, 2005) and some ultrastructural evidence supports the redistribution of cytoplasmic material, most likely soluble crystallins and crystallin fragments, through damaged membranes into extracellular spaces where deposits are formed (Costello et al., 1992; Costello et al., 2007a). Biochemical results support the hypothesis that aggregation of crystallins is favored by oxidation, deamidation and truncation leading to conformational changes that promote crystallin insolubility and cataract (Hanson et al., 2000). However the loss of cytoplasmic material by itself remains to be proven.

The scattering discussed in this study encompasses both forward (or low-angle) scattering, which impacts directly on visual deficit, and backward (or high-angle) scattering, which is directly relevant to the clinician’s grading of cataract prior to surgery. The large fluctuations seen in the images of the cytoplasm from some cataractous lenses (figures 2A, figure 3-yellow line, figure 5A) are likely to cause a significant visual disability because of their central location and low scattering angles, even without factoring in the contributions of membranes and especially multilamellar bodies (Costello et al., 2007b). We demonstrated in the current study that advanced cataracts (higher nuclear cataract grades), in general, show increased texturing and scattering. A systematic approach examining several regions within each lens in a number of lenses in the future will permit the creation of a library of fiber cells from different clinical cataract grades and corresponding scattering. Comparison of these with in vivo methods of estimating the optical properties of the aging lens using light scattering as a tool, some of which have been demonstrated before (Thurston et al., 1997), will allow estimates of the contribution of cytoplasmic packing to overall opacity. In particular, this may lead to the refinement of objective clinical cataract grading, taking into account objective measures of both back scattering and forward scattering in the in vivo lens.

Acknowledgements

The authors wish to acknowledge Mr. Harold Mekeel and Mr. Kenji Leonard for their expert technical assistance. This work has been presented in part at the Association for Research in Vision and Ophthalmology (ARVO) conference, 2007, Florida, USA. Research was supported by grants NIH-NEI EY08148 (UNC) and Core Grant EY05722 (Duke University). Dr. S. Johnsen was supported in part by a grant from the National Science Foundation (IOB-0444674).

References

Al-Ghoul KJ, Costello MJ. Fiber cell morphology and cytoplasmic texture in cataractous and normal human lens nuclei. Curr. Eye. Res 1996;15:533–542. [PubMed: 8670754]

Al-Ghoul KJ, Lane CW, Taylor VL, Fowler WC, Costello MJ. Distribution and type of morphological damage in human nuclear age-related cataracts. Exp. Eye. Res 1996;62:237–251. [PubMed: 8690033]

Bassnett S. Lens organelle degradation. Exp. Eye. Res 2002;74:1–6. [PubMed: 11878813]

Benedek GB. Theory of transparency of the eye. Appl. Opt 1971;10:459–473.

Benedek GB. Cataract as a protein condensation disease: the Proctor Lecture. Invest. Ophthalmol. Vis. Sci 1997;38:1911–1921. [PubMed: 9331254]

Bettelheim, FA. Physical basis of lens transparency. In: Maisel, E., editor. The ocular lens: structure, function, and pathology. New York: Marcel Dekker; 1985. p. 265-300.

Bettelheim FA, Paunovic M. Light scattering of normal human lens I. Application of random density and orientation fluctuation theory. Biophys. J 1979;26:85–99. [PubMed: 262413]

Bettelheim FA, Siew EL. Effect of change in concentration upon lens turbidity as predicted by the random fluctuation theory. Biophys. J 1983;41:29–33. [PubMed: 6824751]

Bettelheim FA, Siew EL, Chylack LT Jr. Studies on human cataracts. III. Structural elements in nuclear cataracts and their contribution to the turbidity. Invest. Ophthalmol. Vis. Sci 1981;20:348–354. [PubMed: 7203880]

Brown, NAP.; Bron, AJ. Lens disorders, A clinical manual of cataract diagnosis. Oxford, UK: Butterworth-Heinemann Ltd.; 1996.

Charney E, Brackett FS. The spectral dependence of scattering from a spherical alga and its implications for the state of organization of the light-accepting pigments. Arch. Biochem. Biophys 1961;92:1–12. [PubMed: 13692507]

Chylack LT Jr, Bettelheim FA, Tung WH. Studies on human cataracts. I. Evaluation of techniques of human cataract preservation after extraction. Invest. Ophthalmol. Vis. Sci 1981;20:327–333. [PubMed: 7203878]

Clark, JI. Development and maintenance of lens transparency. In: Albert, DM.; Jakobiec, FA., editors. Principles and Practice of Ophthalmology. Philadelphia, PA, USA: W. B. Saunders; 1994. p. 114-123.

Clark JI. Fourier and power law analysis of structural complexity in cornea and lens. Micron 2001;32:239–249. [PubMed: 11006504]

Costello MJ. Cryo-electron microscopy of biological samples. Ultrastruct. Path 2006;30:361–371. [PubMed: 17090515]

Costello, MJ.; Gilliland, KO.; Metlapally, S.; Ramamurthy, B.; Krishna, PV.; Balasubramanian, D. Buenos Aires, Argentina: XVII International Congress of Eye Research; 2006. Ultrastructure of junctions in nuclei of advanced cataracts from India.

Costello MJ, Gilliland KO, Metlapally S, Ramamurthy B, Krishna PV, Balasubramanian D. Ultrastructural analysis of damage to nuclear fiber cell membranes in advanced cataracts from India. Invest. Ophthalmol. Vis. Sci 2007a;48:4211.

Costello, MJ.; Johnsen, S. Potential sources of light scattering in human age-related nuclear cataracts: Fourier and Mie scattering analysis. XVI International Congress of Eye Research, Sydney, Australia: Elsevier; 2004.

Costello MJ, Johnsen S, Gilliland KO, Freel CD, Fowler WC. Predicted Light Scattering from Particles Observed in Human Age-Related Nuclear Cataracts Using Mie Scattering Theory. Invest. Ophthalmol. Vis. Sci 2007b;48:303–312. [PubMed: 17197547]

Costello, MJ.; Kuszak, AJ. The Types, Morphology and Causes of Cataracts. In: Garner, A.; Klintoworth, GK., editors. Pathobiology of Ocular Disease. 3rd Ed.. New York: Taylor and Francis; 2007. In press

Costello MJ, Oliver TN, Cobo LM. Cellular architecture in age-related human nuclear cataracts. Invest. Ophthalmol. Vis. Sci 1992;33:3209–3227. [PubMed: 1399426]

Dandona L, Dandona R, Srinivas M, Giridhar P, Vilas K, Prasad MN, John RK, McCarty CA, Rao GN. Blindness in the Indian state of Andhra Pradesh. Invest. Ophthalmol. Vis. Sci 2001;42:908–916. [PubMed: 11274066]

Datiles, MB., 3rd; Magno, BV. Cataract: Clinical Types. In: Tasman, WT.; Jaeger, EA., editors. Duane's Clinical Ophthalmology. Philadelphia: Lippincott Williams & Wilkins; 2004. p. Ch 73

Debye P, Bueche AM. Scattering by an inhomogeneous solid. J. Appl. Phys 1949;20:518–525.

Delaye M, Tardieu A. Short-range order of crystallin proteins accounts for eye lens transparency. Nature 1983;302:415–417. [PubMed: 6835373]

Diniz, PSR.; da Silva, EAB.; Netto, SL. Digital Signal Processing: System Analysis and Design. Meyler, P.; Willner, E., editors. Cambridge University Press; 2002.

Duncan, G. On Classifying Human Cataractous Lenses. In: Duncan, G., editor. Mechanisms of Cataract Formation in the Human Lens. London and New York: Academic Press; 1981. p. 1-5.

Foster A. Cataract and "Vision 2020-the right to sight" initiative. Br. J. Ophthalmol 2001;85:635–637. [PubMed: 11371475]

Freegard TJ. The physical basis of transparency of the normal cornea. Eye 1997;11(Pt 4):465–471. [PubMed: 9425408]

Freel CD, Gilliland KO, Mekeel HE, Giblin FJ, Costello MJ. Ultrastructural characterization and Fourier analysis of fiber cell cytoplasm in the hyperbaric oxygen treated guinea pig lens opacification model. Exp. Eye. Res 2003;76:405–415. [PubMed: 12634105]

Freel CD, Gilliland KO, Wesley Lane C, Giblin FJ, Joseph Costello M. Fourier analysis of cytoplasmic texture in nuclear fiber cells from transparent and cataractous human and animal lenses. Exp. Eye. Res 2002;74:689–702. [PubMed: 12126943]

Gilliland KO, Freel CD, Johnsen S, Craig Fowler W, Costello MJ. Distribution, spherical structure and predicted Mie scattering of multilamellar bodies in human age-related nuclear cataracts. Exp. Eye. Res 2004;79:563–576. [PubMed: 15381040]

Gilliland KO, Freel CD, Lane CW, Fowler WC, Costello MJ. Multilamellar bodies as potential scattering particles in human age-related nuclear cataracts. Mol. Vis 2001;7:120–130. [PubMed: 11435998]

Gisselberg M, Clark JI, Vaezy S, Osgood TB. A quantitative evaluation of Fourier components in transparent and opaque calf cornea. Am. J. Anat 1991;191:408–418. [PubMed: 1951139]

Glauert, AM. Section staining, cytology, autoradiography, and immunochemistry for biological specimens. In: Kay, DH., editor. Techniques for Electron Microscopy. Oxford: Blackwell; 1965. p. 254-310.

Hanson SR, Hasan A, Smith DL, Smith JB. The major in vivo modifications of the human water-insoluble lens crystallins are disulfide bonds, deamidation, methionine oxidation and backbone cleavage. Exp. Eye. Res 2000;71:195–207. [PubMed: 10930324]

Hayat, MA. Principles and Techniques of Electron Microscopy: Biological Applications. vol. 1. New York: Van Nostrand Reinhold; 1971.

Jedziniak JA, Kinoshita JH, Yates EM, Benedek GB. The concentration and localization of heavy molecular weight aggregates in aging normal and cataractous human lenses. Exp. Eye. Res 1975;20:367–369. [PubMed: 1126401]

Jedziniak JA, Kinoshita JH, Yates EM, Hocker LO, Benedek GB. On the presence and mechanism of formation of heavy molecular weight aggregates in human normal and cataractous lenses. Exp. Eye. Res 1973;15:185–192. [PubMed: 4692231]

Kenworthy AK, Magid AD, Oliver TN, McIntosh TJ. Colloid osmotic pressure of steer alpha- and beta-crystallins: possible functional roles for lens crystallin distribution and structural diversity. Exp. Eye. Res 1994;59:11–30. [PubMed: 7835391]

Kramps HA, Stols AL, Hoenders HJ. On the quaternary structure of high-molecular-weight proteins from the bovine eye lens. Eur. J. Biochem 1975;50:503–509. [PubMed: 1112267]

Kuszak, JR.; Al-Ghoul, KJ.; Costello, MJ. Pathology of age-related human cataracts. In: Tasman, WT.; Jaeger, EA., editors. Duane's Clinical Ophthalmology. vol. 71B. Philadelphia: Lippincott Williams & Wilkins; 1998. p. 1-14.

Kuszak, JR.; Costello, MJ. The Structure of the Vertebrate Lens. In: Lovicu, FJ.; Robinson, ML., editors. Development of the Ocular Lens. Cambridge, UK: Cambridge Univ. Press; 2004. p. 71-118.

Lampi KJ, Ma Z, Hanson SR, Azuma M, Shih M, Shearer TR, Smith DL, Smith JB, David LL. Age-related changes in human lens crystallins identified by two-dimensional electrophoresis and mass spectrometry. Exp. Eye. Res 1998;67:31–43. [PubMed: 9702176]

Liem-The KN, Stols AL, Hoenders HJ. Further characterization of HM-crystallin in rabbit lens. Exp. Eye. Res 1975;20:307–316. [PubMed: 1126398]

Ma Z, Hanson SR, Lampi KJ, David LL, Smith DL, Smith JB. Age-related changes in human lens crystallins identified by HPLC and mass spectrometry. Exp. Eye. Res 1998;67:21–30. [PubMed: 9702175]

Marsili S, Salganik RI, Albright CD, Freel CD, Johnsen S, Peiffer RL, Costello MJ. Cataract formation in a strain of rats selected for high oxidative stress. Exp. Eye. Res 2004;79:595–612. [PubMed: 15500819]

McGinty SJ, Truscott RJ. Presbyopia: the first stage of nuclear cataract? Ophthalmic. Res 2006;38:137–148. [PubMed: 16397406]

Michielsen, S. Specific refractive index increments of polymers in dilute solution. In: Brandup, J.; Immergut, EH.; Grulke, EA., editors. Polymer Handbook. 4th Ed.. New York: Wiley; 1999. p. 547-628.

Murthy GV, Gupta SK, Maraini G, Camparini M, Price GM, Dherani M, John N, Chakravarthy U, Fletcher AE. Prevalence of lens opacities in North India: the INDEYE feasibility study. Invest. Ophthalmol. Vis. Sci 2007;48:88–95. [PubMed: 17197521]

Nirmalan PK, Krishnadas R, Ramakrishnan R, Thulasiraj RD, Katz J, Tielsch JM, Robin AL. Lens opacities in a rural population of southern India: the Aravind Comprehensive Eye Study. Invest. Ophthalmol. Vis. Sci 2003;44:4639–4643. [PubMed: 14578379]

Philipson B. Changes in the lens related to the reduction of transparency. Exp. Eye. Res 1973;16:29–39. [PubMed: 4718699]

Siew EL, Bettelheim FA, Chylack LT Jr, Tung WH. Studies on human cataracts. II. Correlation between the clinical description and the light-scattering parameters of human cataracts. Invest. Ophthalmol. Vis. Sci 1981;20:334–347. [PubMed: 7203879]

Siezen RJ, Bindels JG, Hoenders HJ. The interrelationship between monomeric, oligomeric and polymeric alpha-crystallin in the calf lens nucleus. Exp. Eye. Res 1979;28:551–567. [PubMed: 446575]

Spector A, Roy D. Disulfide-linked high molecular weight protein associated with human cataract. Proc. Natl. Acad. Sci. USA 1978;75:3244–3248. [PubMed: 277922]

Tardieu A, Veretout F, Krop B, Slingsby C. Protein interactions in the calf eye lens: interactions between beta-crystallins are repulsive whereas in gamma-crystallins they are attractive. Eur. Biophys 1992;21:1–12.

Taylor VL, Al-Ghoul KJ, Lane CW, Davis VA, Kuszak JR, Costello MJ. Morphology of the normal human lens. Invest. Ophthalmol. Vis. Sci 1996;37:1396–1410. [PubMed: 8641842]

Taylor VL, Costello MJ. Fourier analysis of textural variations in human normal and cataractous lens nuclear fiber cell cytoplasm. Exp. Eye. Res 1999;69:163–174. [PubMed: 10433853]

Taylor VL, Peiffer RL, Costello MJ. Ultrastructural analysis of normal and diabetic cataractous canine lenses. Vet. & Comp. Ophthalmol 1997;7:117–125.

Thurston GM, Hayden DL, Burrows P, Clark JI, Taret VG, Kandel J, Courogen M, Peetermans JA, Bowen MS, Miller D, Sullivan KM, Storb R, Stern H, Benedek GB. Quasielastic light scattering study of the living human lens as a function of age. Curr. Eye. Res 1997;16:197–207. [PubMed: 9088735]

Thylefors B, Negrel AD, Pararajasegaram R, Dadzie KY. Global data on blindness. Bull. World. Health. Organ 1995;73:115–121. [PubMed: 7704921]

Truscott RJ. Age-related nuclear cataract-oxidation is the key. Exp. Eye. Res 2005;80:709–725. [PubMed: 15862178]

Vaezy S, Clark JI. Quantitative analysis of the microstructure of the human cornea and sclera using 2-D Fourier methods. J. Microsc 1994;175:93–99. [PubMed: 7966254]

Vaezy S, Clark JI. Characterization of the cellular microstructure of ocular lens using 2D power law analysis. Ann. Biomed. Eng 1995;23:482–490. [PubMed: 7486355]

Vaezy S, Clark JI, Clark JM. Quantitative analysis of the lens cell microstructure in selenite cataract using a two-dimensional Fourier analysis. Exp. Eye. Res 1995;60:245–255. [PubMed: 7789405]

van den Berg TJ. Light scattering by donor lenses as a function of depth and wavelength. Invest. Ophthalmol. Vis. Sci 1997;38:1321–1332. [PubMed: 9191595]

Zigler, JS. Lens proteins. In: Albert, DM.; Jakobiec, FA., editors. Principles and Practice of Ophthalmology. Philadelphia, PA, USA: W.B. Saunders & Co; 1994. p. 97-113.

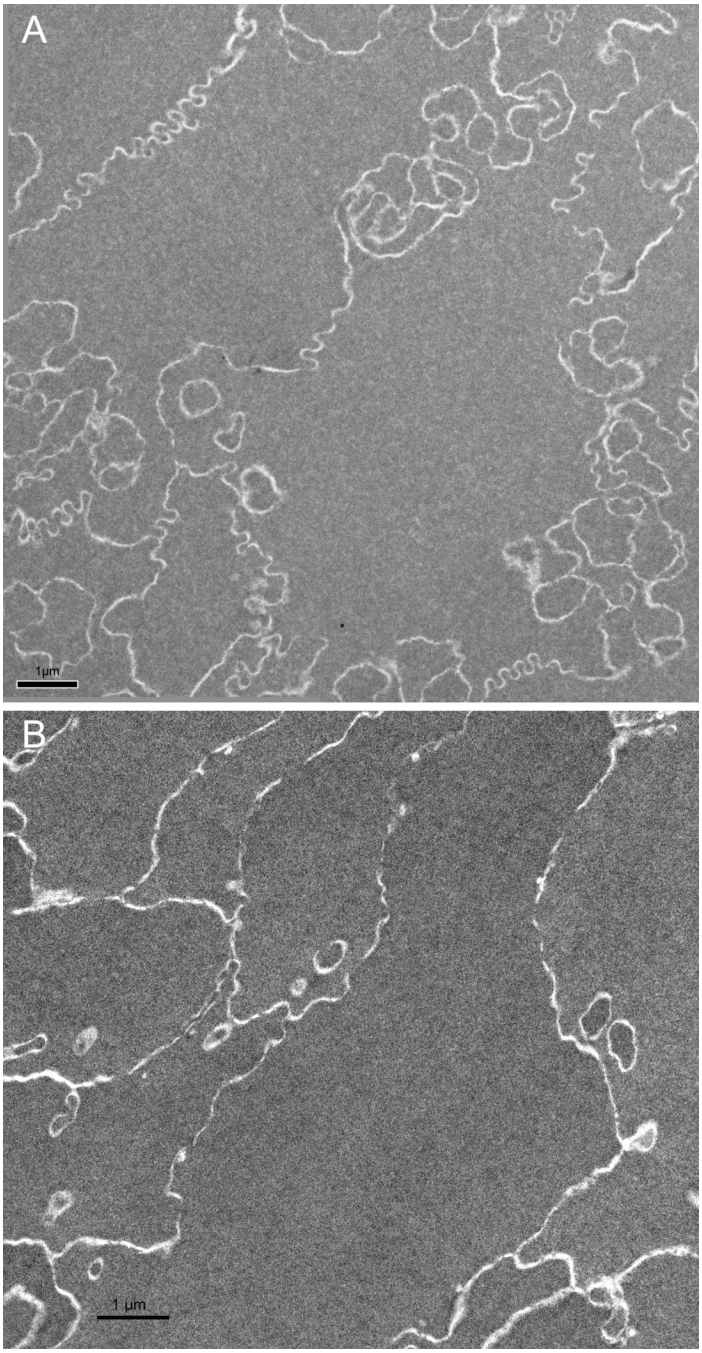

Figure 1.
Low magnification micrographs from representative advanced cataractous and transparent human lenses appear similar. Equivalent regions from these two types of lenses (A) and (B), aged 75 and 56 years, respectively, in this illustration, appear essentially the same with respect to membrane profiles and cytoplasmic textures visible by eye and no obvious damage is evident. Scale bars are 1 μm.

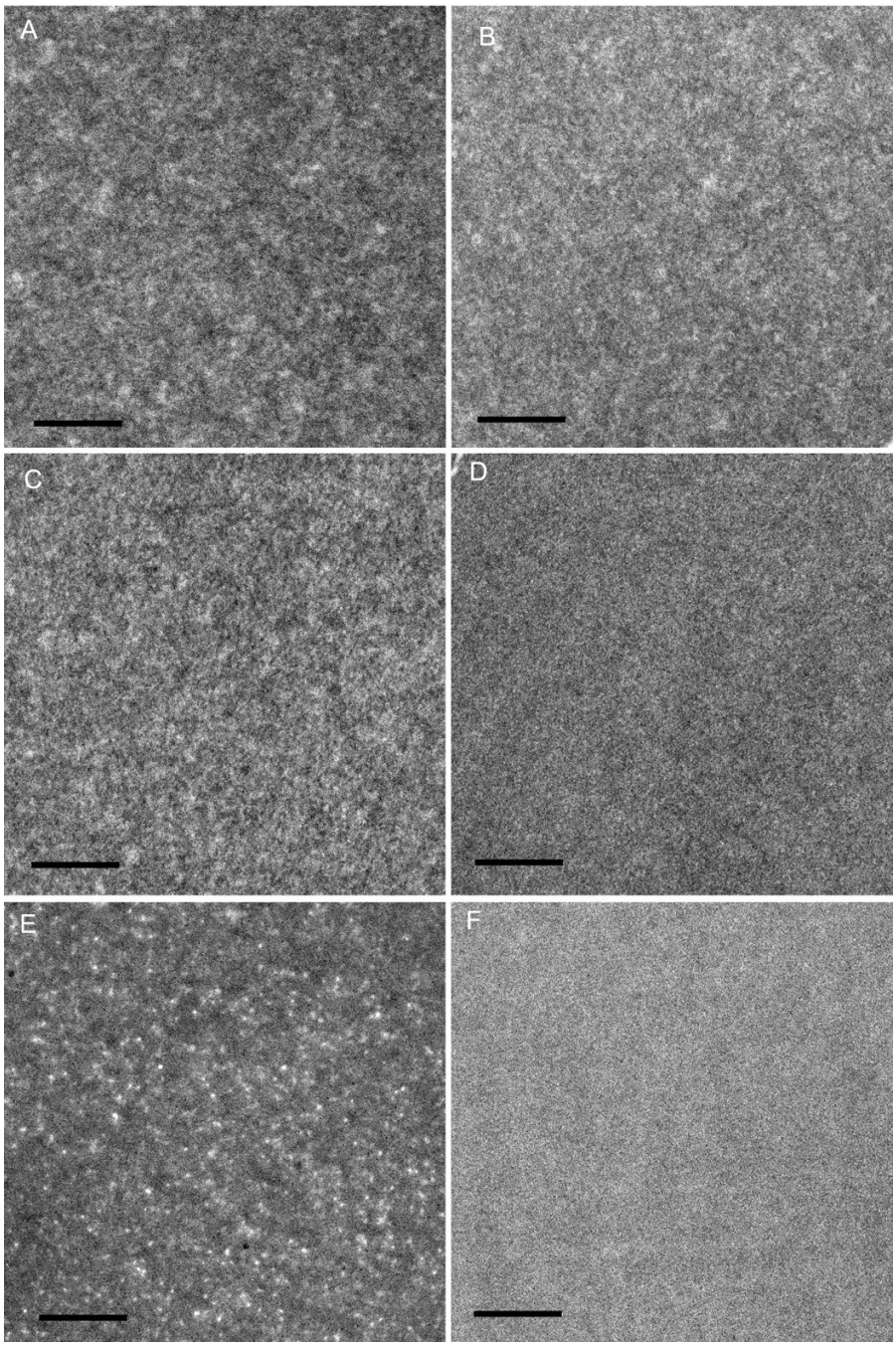

Figure 2.
Higher magnification images from human lenses and comparable regions in OXYS and normal rat lenses reveal qualitative differences in cytoplasmic textures. Images collected at 6500X for analysis of scattering revealed visible differences with human advanced cataracts from India (A, B, C) and OXYS rat (E) lenses showing highly textured cytoplasms followed by the relatively smooth texture seen in human transparent lenses from India (D). Normal rat lenses (F) had the smoothest texture compared to the rest of the lenses examined in this study. Scale bars are 0.5 μm.

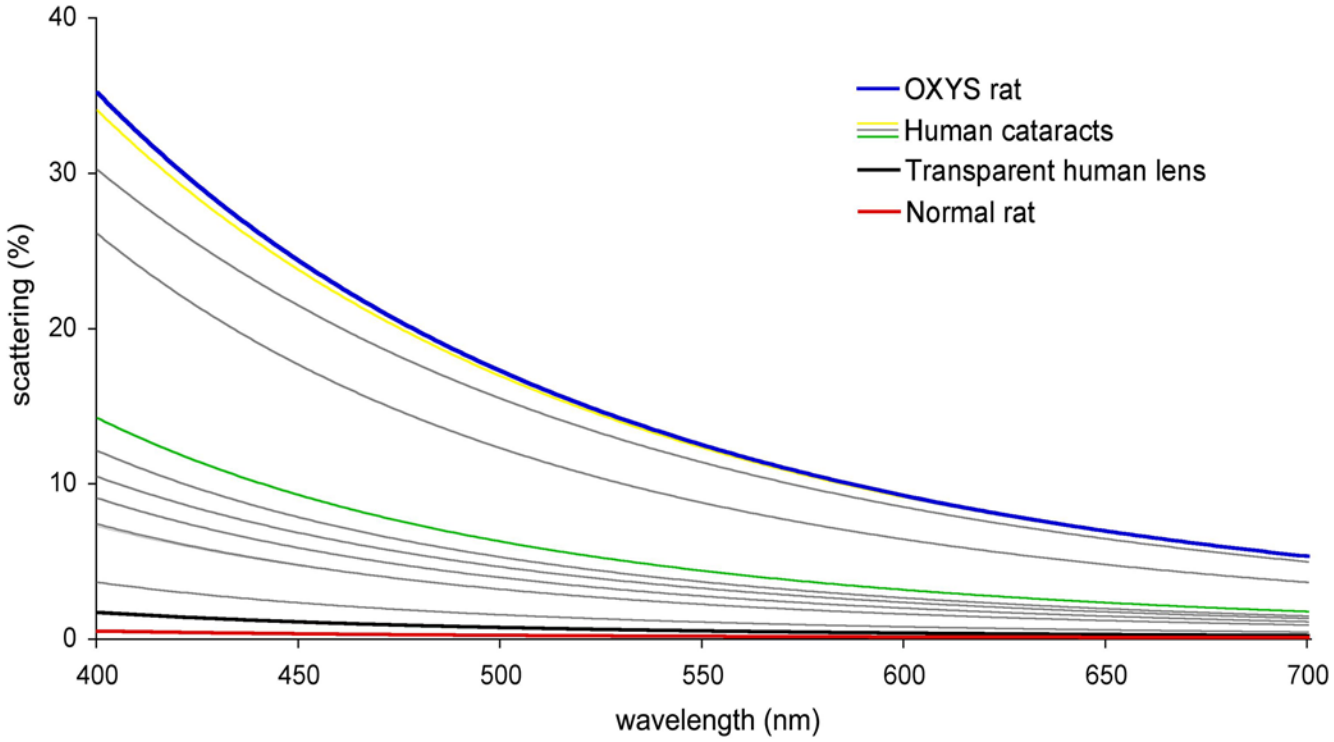

Figure 3.

Percent scattering plotted against wavelength of visible light for representative cells from all the lenses. Cataracts from India revealed significantly higher scattering from the cytoplasm of their innermost cells compared to transparent donor lenses. Scattering from the OXYS rat was the highest and concurred with the cytoplasmic texture visible by eye and with earlier findings. Normal rat lenses with the smoothest texture showed the least scattering. The yellow line, the grey line immediately below it and the green line were calculated from the images of cytoplasm from cataracts shown in figures 2A, 2B and 2C, respectively. The transparent human lens represented by the black line was calculated from the image shown in figure 2D. Calculations for percent scatter in the OXYS and normal rat were made from images 2E and 2F, respectively.

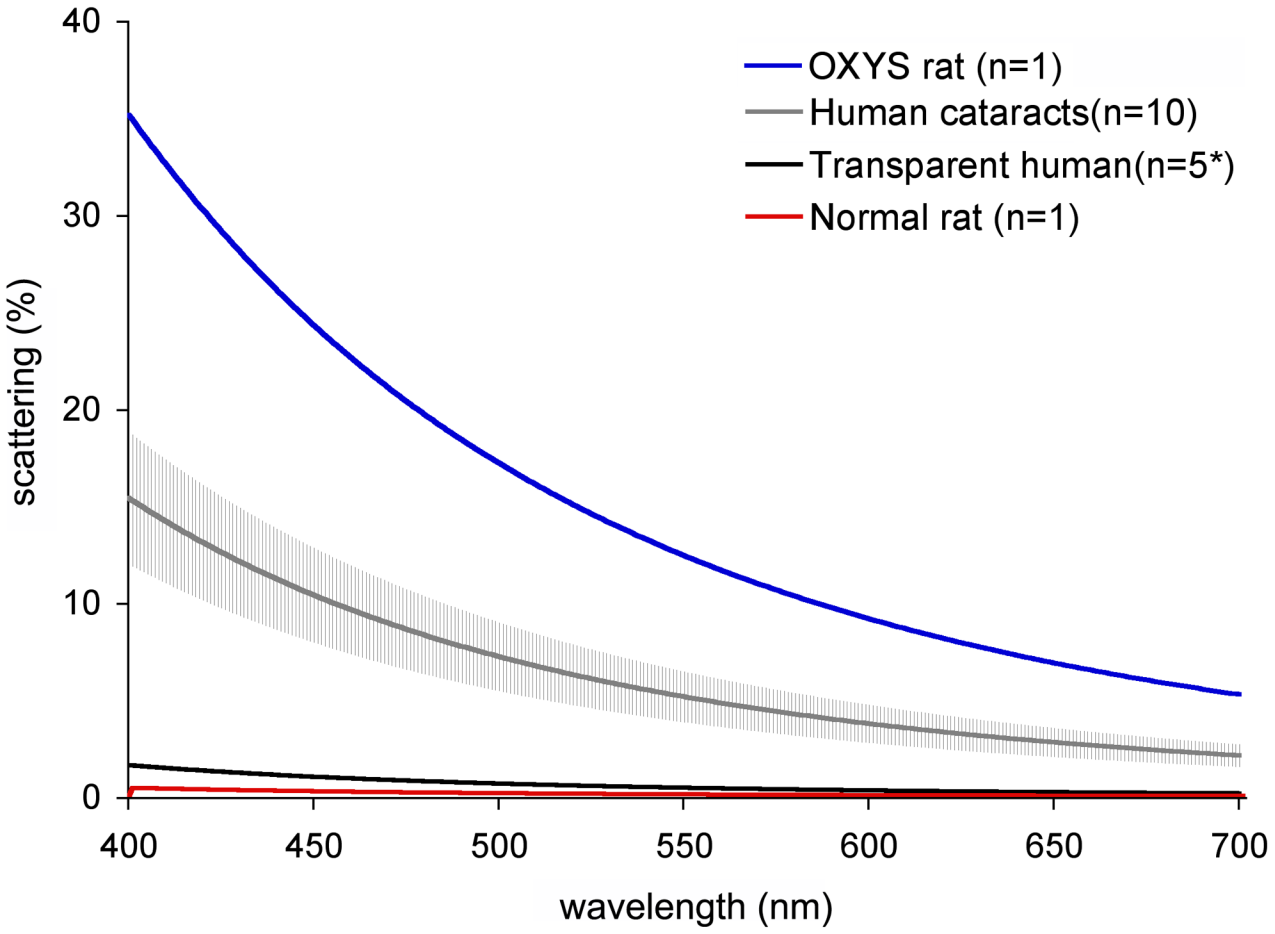

Figure 4.
Average percent scattering plotted against wavelength of visible light. Data from the ten cataracts were averaged and compared with the average percent scattering from transparent donor lenses (*error bars not computed for the transparent lens because 5 cells from the same lens were used to obtain the average percent scatter). Cataractous lenses revealed considerably higher scattering than transparent lenses from India. Error bars represent ± standard error.

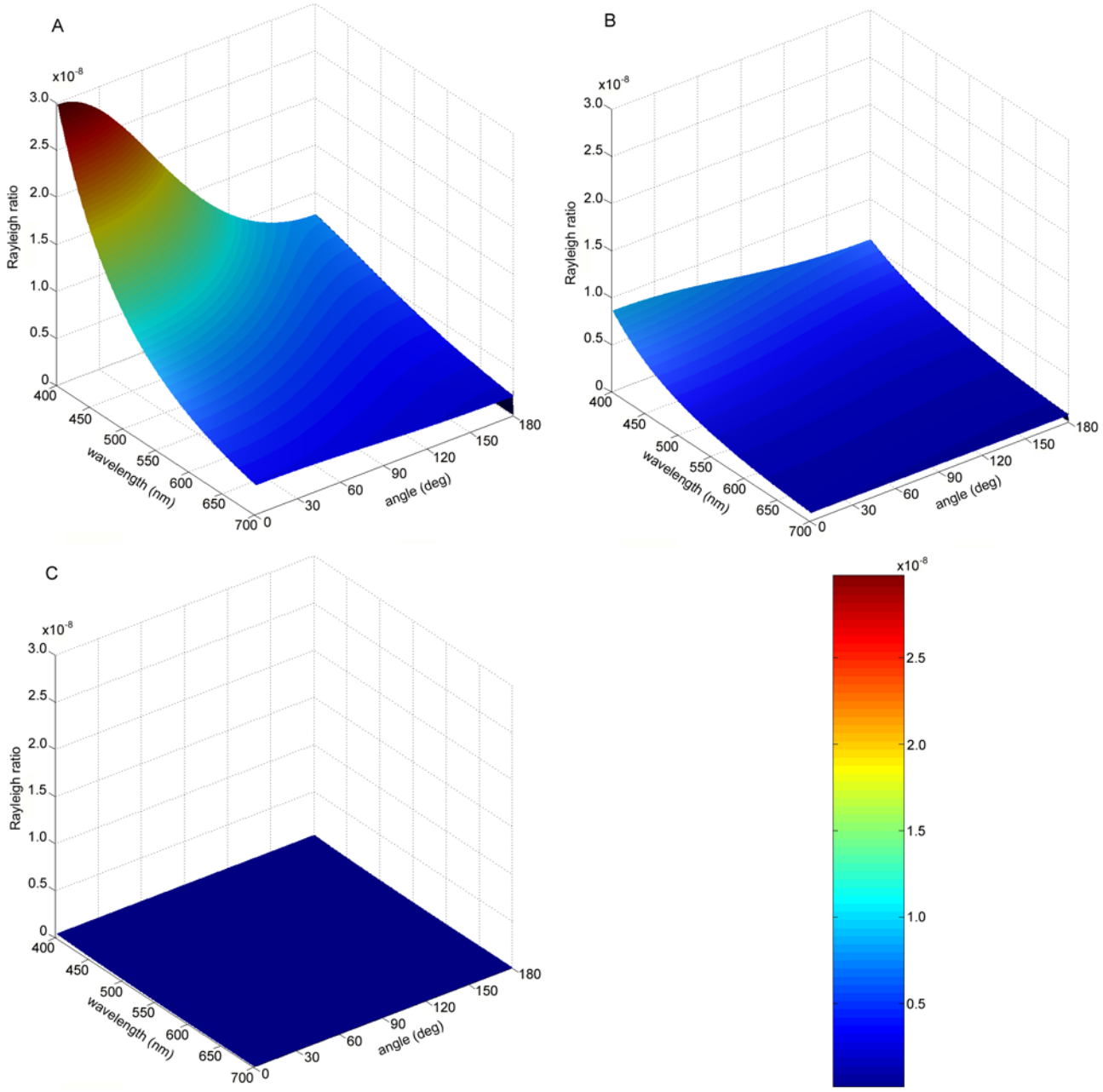

Figure 5.

Scattering exhibited as Rayleigh ratios plotted against scattering angle and wavelength. Two different cataracts and a transparent human lens were plotted as three dimensional graphs. A. The lens exhibiting the highest percent scattering (also figure 2A and yellow line in figure 3) shows large-scale fluctuations that cause considerable opacity and represent large density fluctuations, as implied by the high scattering at low scattering angles. B. A different cataractous lens representing medium scattering (also figure 2C and green line in figure 3) and C. a transparent donor lens (also figure 2D and black line in figure 3) are also shown for comparison. Scattering is represented as Rayleigh ratios which are the ratios of scattered intensity to incident intensity times the ratio of the squared distance to the detector over the

volume of the sample. The use of Rayleigh ratios enhances comparisons because polarization effects and scattering geometry are automatically taken into account.